UAV Trajectory Prediction Based on Flight State Recognition

JIANDONG ZHANG
ZHUOYONG SHI
Northwestern Polytechnical University, Xi'an, China

ANLI ZHANG
Xi'an Jiaotong University City College, Xi'an, China

QIMING YANG
GUOQING SHI
YONG WU
Northwestern Polytechnical University, Xi'an, China

UAV trajectory prediction is the core technology for autonomous UAV flight and is a prerequisite for control and navigation. In this article, the UAV flight path prediction model is established by collecting the flight data of the actual UAV. First, the UAV flight information collection and data preprocessing are carried out; second, the UAV flight state recognition model is established based on the PCA-SVM model to identify five UAV flight states; and finally, the flight path prediction model of UAV based on flight state recognition is established, and the neural network model is established based on the flight path of five flight state recognition. The experimental results show that: first, the accuracy of UAV flight state recognition based on PCA-SVM is more than 90%; second, the average prediction error of the traditional neural network UAV trajectory is 0.422 m, and the maximum error of the circling state is 0.84 m; and third, the average prediction error of the UAV flight path based on flight state recognition is 0.214 m, and the maximum error of the circling state is 0.41 m. The model error is less than 0.5 m. The results show that the prediction model with flight state recognition has significantly less error than the direct UAV trajectory prediction, and the prediction model with flight state recognition predicts better than the traditional unscented Kalman filter method.

Manuscript received 6 February 2023; revised 25 May 2023 and 23 June 2023; accepted 6 August 2023. Date of publication 10 August 2023; date of current version 11 June 2024.

DOI. No. 10.1109/TAES.2023.3303854

Refereeing of this contribution was handled by J. Dunik.

This work was supported in part by the Natural Science Basic Research Program of Shaanxi under Grant 2022JQ-593 and in part by the Key R&D Program of Shaanxi Provincial Department of Science and Technology under Grant 2022GY-089.

Authors' addresses: Jiandong Zhang, Zhuoyong Shi, Qiming Yang, Guoqing Shi, and Yong Wu are with the School of Electronics and Information, Northwestern Polytechnical University, Xi'an 710129, China, E-mail: (jdzhang@nwpu.edu.cn; shizy@mail.nwpu.edu.cn; yangqm1988@163.com; shiguoqing@nwpu.edu.cn; yongwu@nwpu.edu.cn); Anli Zhang is with the Department of Electrical and Information Engineering, Xi'an Jiaotong University City College, Xi'an 710018, China, E-mail: (79213880@qq.com). *(Corresponding author: Zhuoyong Shi.)*

0018-9251 © 2023 IEEE

NOMENCLATURE

UAV	Unmanned aerial vehicle.
SVM	Support vector machine.
PCA	Principal component analysis.
UKF	Unscented Kalman filter.
CPU	Central processing unit.
GPS	Global positioning system.
PC	Personal computer.
MSE	Mean square error.

I. INTRODUCTION

UAV is an unmanned aerial vehicle that flies by radio remote control or executes its program [1], [2]. It has the advantages of convenient deployment, strong maneuverability, and low cost. UAVs are of great value in military, civilian, and commercial fields. In the military field, UAVs can be used to complete tasks including reconnaissance, target positioning, intelligence search, and decoy fire [3]. In the civilian field, UAVs can complete high-altitude and high-risk tasks such as express transportation, pesticide spraying, and antenna inspection [4], [5]. In the commercial field, UAVs can complete aerial photography from various angles to capture better-angle photography [6], [7]. With the rapid rise of the field of UAVs, its safety problems have become increasingly prominent, and the UAV safety supervision system has emerged [8], [9]. The trajectory prediction of UAVs is the core technology of UAV safety supervision [10], [11], [12], and it is a necessary condition to realize a more automatic and accurate UAV supervision system. The trajectory prediction of a UAV refers to the process of estimating the future trajectory of the UAV through the local information of the UAV [13]. The trajectory prediction of the UAV can provide more accurate navigation data for the control and navigation of the UAV.

At present, there are mainly three methods for UAV trajectory prediction: hybrid estimation, particle motion model, and machine learning.

The hybrid estimation algorithm was first applied to the field of positioning and trajectory tracking, mainly including the Kalman filter and particle filter. de Marina et al. [14] proposed an attitude and heading reference system based on an UKF, and verified the effectiveness of the method with UAV. Kannan et al. [15] proposed a novel sensor fusion estimation method based on a low-complexity linear Kalman filter based on the differential state equation, which improved the prediction accuracy and response time.

The UAV particle motion model regards the UAV as a moving particle during the movement process, ignores the rolling motion of the UAV, and uses the full energy equation to construct the UAV trajectory module [16]. The

Authorized licensed use limited to: Pontificia Universidad Catolica de Chile. Downloaded on March 20,2025 at 19:23:50 UTC from IEEE Xplore. Restrictions apply.

particle motion model depicts the 4-D trajectory of the UAV based on the particle motion of the UAV. Thipphavong and Schultz [17] analyzed the performance of a trajectory-based automatic separation assurance system under different uncertainty conditions, which was able to identify 99% of high-altitude conflicts. Zhang et al. [18] designed a combined 4-D trajectory prediction model based on historical flight data and UAV equations of motion, and used a genetic algorithm to dynamically weight this prediction model. Simulation experiments showed that the model was able to accurately predict the flight trajectory of the UAV and the time to enter the protected area in real time, but it was not sufficiently considered in the dynamic characteristics of the UAV. Niu et al. [19] designed an adjacent motion trajectory prediction algorithm based on model predictive control (MPC) to enable a single UAV to predict adjacent motion trajectories without communication. The effectiveness of the MPC algorithm proposed in the article in multilevel trajectory planning was also verified based on the distributed MPC framework. However, the algorithm is still at the simulation level and has not been put to test in a real UAV.

Based on a machine learning approach, the current UAV's trajectory is predicted by learning the onboard data and trajectory changes during the UAV's historical navigation. Alligier and Gianazza [20] used the gradient boosting algorithm to predict parameters such as the mass velocity intent of the particle model, which improved the prediction accuracy of the UAV in the climbing state. Wang et al. [21] divided the motion of the UAV into various motion states, used the Gaussian process regression (GPR) algorithm to learn the state transition model, combined the UKF for trajectory prediction, and verified the accuracy of the algorithm through real flight data. Kada et al. [22] used the UKF and the minimum energy Kalman filter to solve the UAV attitude estimation problem. Zhong et al. [23] designed a UAV trajectory prediction model based on long short-term memory network to improve the trajectory prediction accuracy of UAVs with random behavioral intentions and tested the method to obtain better prediction accuracy in a shorter prediction time range (0–3 s). Liu et al. [24] proposed a new time-series convolutional neural network (TSCNN) based on deep learning trajectory mapping network to improve the efficiency of the trajectory prediction model, after testing, compared to other deep learning models in terms of computation time and prediction accuracy TSCNN has better performance in both metrics. Xie and Chen [25] proposed a GPR framework for UAV trajectory prediction, which enables online prediction of UAV trajectories, and simulations and real datasets demonstrate that the proposed framework outperforms competing trajectory prediction methods.

The above kinds of literature all conduct prediction studies on the UAV flight path itself, focusing on the prediction of the future UAV flight path from the historical UAV flight path. Most studies focus on the optimization of the UAV flight path prediction algorithm, and the influence of the current UAV flight state on the UAV flight path is weakened or insufficient to a certain extent. In this article, a UAV flight trajectory prediction model is established to classify and identify the flight status of UAVs, and the reliability of the prediction model is verified based on actual UAV flight trajectory data. On this basis, a neural network is established to predict the UAV flight path according to different flight states. After classification and identification of UAV flight status, the UAV flight path prediction can clarify the prediction target and further improve the accuracy of UAV flight path prediction.

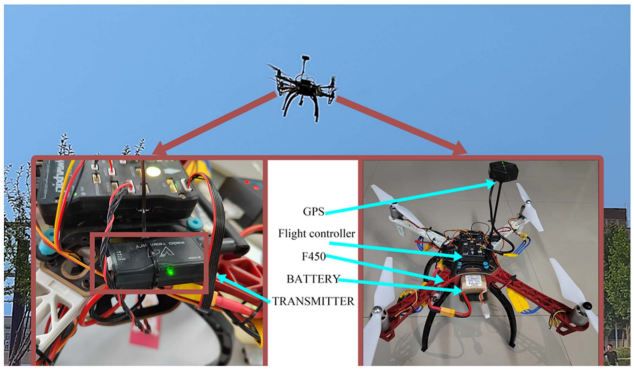

Fig. 1. UAV information collection system.

The direct application of traditional machine learning methods in UAV flight trajectory prediction cannot specifically consider the impact of UAV flight states on its flight trajectory. Therefore, the introduction of a flight state recognition process for deep learning prediction of UAV flight paths for different flight states can improve the accuracy of UAV machine learning. In this article, a UAV trajectory prediction model based on flight state recognition is proposed, which is mainly used for flight control during the autonomous flight of UAVs, etc. This article first collects and processes the UAV data, then identifies the UAV flight states, and finally builds a UAV trajectory prediction model based on the different flight states of the UAV to achieve UAV trajectory prediction.

II. DATA ACQUISITION AND PROCESSING

A. UAV Data Acquisition

Fig. 1 shows a system of UAV data collection by GPS, Flight controller, F450, BATTERY, TRANSMITTER, etc. The GPS collects the airborne information of the UAV, the Flight controller controls the operation of the whole system, the F450 is the body module of the UAV, the BATTERY is the system power module that supplies power to the whole system, and the TRANSMITTER is the data transmitter module that transmits the collected information to the ground.

The TRANSMITTER system is built with a 3DR wireless digital transmission station, and the structure of the 3DR wireless digital transmission station is shown in Fig. 2. In Fig. 2, a diagram of the UAV's communication with the PC via the 3DR wireless data transmission system is depicted. The RX stands for Receive, which is the receiver of the data in the device; the TX stands for Transmit, which is the sender of the data in the device; and the GND stands for Ground, which is the common 0 line in the device.

Authorized licensed use limited to: Pontificia Universidad Catolica de Chile. Downloaded on March 20,2025 at 19:23:50 UTC from IEEE Xplore. Restrictions apply.

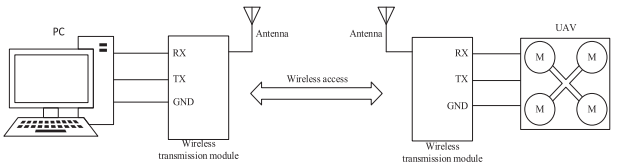

Fig. 2. UAV digital transmission system.

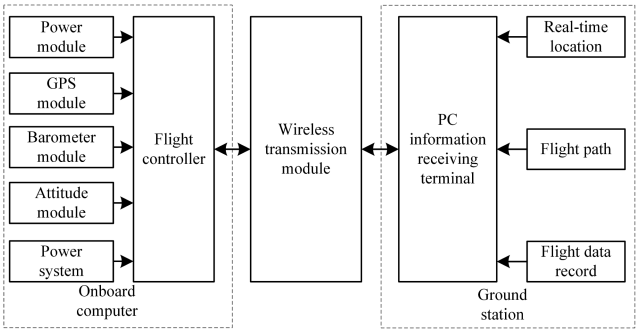

Fig. 3. UAV information acquisition system structure block diagram.

TABLE I
Acquisition Data of UAV

Data Name	Data Volume	Time Resolution
GPS Data	10 000	0.1 s
Angular Velocity Data	10 000	0.1 s
Acceleration Data	10 000	0.1 s
Barometer Data	10 000	0.1 s

The structure block diagram of the UAV information collection system built in this study is shown in Fig. 3. The onboard computer, including power module, GPS module, barometer module, attitude module, power system, is controlled by the Flight controller. At the same time, the onboard computer communicates with the PC side of the Ground station through the wireless transmission module to achieve data transmission of the UAV system.

Through the UAV data acquisition system shown in Fig. 3, the data collected during the flight of the UAV are used to support this study. The UAV data collected are shown in Table I.

As shown in Table I, with the data name UAV GPS information, angular velocity information, acceleration information, and barometer information, the amount of data collected is 10 000, and the time resolution of the collection is 0.1 s.

B. Data Preprocessing

The collected UAV trajectory data may generate noise due to instrument acquisition or data transmission, so it is necessary to perform data preprocessing before UAV data analysis. The data preprocessing mainly includes the rejection of abnormal data, the repair of missing data and the filtering of high-frequency noise, and the output of the repaired data after the repair is completed.

1) *Abnormal Data Rejection:* For a set of data n samples $\{x_1, x_2, \ldots, x_n\}$ returned by the UAV, after returning the data, the first-order difference $X_i$is calculated as shown in the following formula:

$$X_i = x_{i+1} - x_i \, (i = 1, 2, \ldots, n-1). \tag{1}$$

In formula (1), X_i describes the change of the corresponding data of the UAV over a period of time. According to statistical knowledge, the change should be within a certain interval, and the data are eliminated by counting the statistical characteristics of X_i.

The mathematical expectation of the first-order difference data $X_i$of the UAV flight sample x_i is shown in the following formula:

$$EX = \frac{1}{n-1} \sum_{i=1}^{n-1} X_i. \tag{2}$$

The standard deviation σ of the first-order difference data X_i is shown in the following formula:

$$\sigma = \sqrt{\frac{1}{n-1} \sum\nolimits_{i=1}^{n-1} (X_i - EX)^2}. \tag{3}$$

According to statistical principles, the first-order difference X_i of the data sample obeys a normal distribution. According to the 3σ criterion, the data in the $(EX - 3\sigma, EX + 3\sigma)$ interval in X_i are retained, the data outside the interval are considered to be abnormal data and eliminated, and the X_i abnormal data outside the interval and the corresponding x_{i+1} data are eliminated, to realize the elimination of abnormal data.

2) *Missing Data Repair:* After the outliers are taken out, the data are arranged and combined, and the missing data are interpolated and smoothed by the Lagrange interpolation method, and finally the repaired data are output.

For a set of data after removing outliers, its permutation is denoted as $(x_0, y_0), \ldots, (x_k, y_k)$, x_j represents the position of the independent variable, y_j represents the value of the function at this position, and all x_j are different; then, according to the Lagrange interpolation formula, the polynomial of Lagrange interpolation can be obtained as shown in the following equation:

$$L(x) = \sum_{j=0}^{k} y_j l_j(x). \tag{4}$$

Among them, each $l_j(x)$ is a Lagrange fundamental polynomial, and the expression is shown in the following formula:

$$l_j(x) = \prod_{i=0, i \neq j}^{k} \frac{x - x_i}{x_j - x_i}. \tag{5}$$

Using the fitted Lagrange polynomial as the estimation of the curve, inputting the data position of the missing value into the polynomial can predict the value of the function at this position, so as to realize the data interpolation estimation of the missing data position.

3) *High-Frequency Noise Filtering:* Based on that, an adaptive smoothing filtering method is used to update the filtering parameters by increasing the threshold value in order to adapt to the real-time signal. The new output value is

Authorized licensed use limited to: Pontificia Universidad Catolica de Chile. Downloaded on March 20,2025 at 19:23:50 UTC from IEEE Xplore. Restrictions apply.

TABLE II
Motion Parameters of UAV During Flight

Data name	Definition	Calculation formula	
altitude	Altitude of UAV in space	$z = 4.43\times10^{4}\times(1-9.87\times10^{-6}P)^{\frac{1}{5.256}}$	(7)
speed	Change rate of UAV position with time	$\begin{cases} v_x = \frac{\Delta x}{\Delta t} \\ v_y = \frac{\Delta y}{\Delta t} \\ v_z = \frac{\Delta z}{\Delta t} \end{cases}$	(8)
acceleration	Change rate of UAV speed with time	$\begin{cases} a_x = \frac{\Delta v_x}{\Delta t} \\ a_y = \frac{\Delta v_y}{vt} \\ a_z = \frac{\Delta v_z}{\Delta t} \end{cases}$	(9)
direction	Travel direction in UAV plane	$\theta = \arctan\frac{v_y}{v_x}$	(10)
curvature	Curved degree of UAV motion curve	$K = \frac{\Delta a}{\Delta s}$	(11)

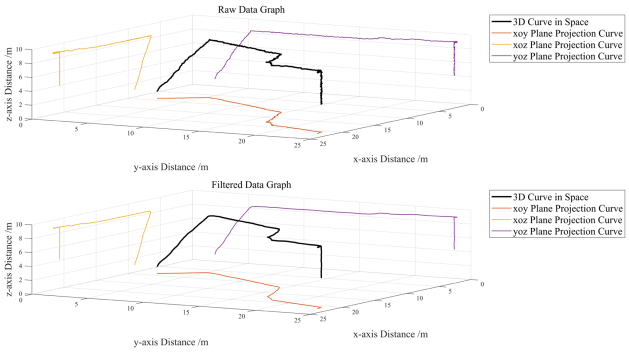

Fig. 4. Data preprocessing image.

defined as the current sample value and the previous output value is weighted to obtain the current output value. The filtered output is shown in the following formula:

$$Y(n) = m \cdot X(n) + (1 - m) \cdot Y(n - 1) \tag{6}$$

where $Y(n)$ is the filter output value, m is the filter coefficient between the interval [0, 1], $X(n)$ is the current sample value, and $Y(n - 1)$ is the previous filter output value.

As can be seen in formula (6), the filter coefficient is the most important parameter of the filter and has a great impact on the filtering effect. In order to make the filter design more reasonable, the time-varying characteristics of the input signal are analyzed in trajectories and the filter parameters are updated at the signal output.

Data preprocessing is performed on a section of the UAV flight trajectory, and the processing effect is shown in Fig. 4.

Fig. 4 shows that the error signals generated during the acquisition process can be better filtered out after data preprocessing.

C. Related Data Solution

The motion parameters of UAVs during flight mainly include position, velocity, acceleration, direction, curvature, etc., in space. The space position of the UAV can be obtained by converting the air pressure data to the z-axis position, and combined with the plane position, the space position of the UAV can be obtained. The space velocity of UAV is obtained by the first-order difference of UAV position; the space acceleration of UAV is obtained by the first-order difference of velocity. The direction of UAV is defined as the forward direction of plane space, and its tangent value is obtained through the ratio of velocity. The curvature of a UAV is defined as the ratio of the angle of rotation of the UAV to the length of the arc. The definition and calculation formula of position, velocity, acceleration, direction, curvature, etc., in UAV space are shown in Table II.

As shown in Table II, the definition of position, velocity, acceleration, direction, curvature, and other motion parameters in space during UAV flight and their calculation formulas are described.

III. UAV FLIGHT STATUS RECOGNITION MODEL

A. UAV Trajectory Feature Construction

The dimension of UAV original data is high. In the field of machine learning, overlearning directly affects the classification accuracy [26]. Therefore, it is necessary to reduce the dimension of data. PCA, as a dimension reduction algorithm, can reduce multiple indicators to several principal components. They are linear combinations of original variables without any relationship between them, which can reflect most of the useful information in the original data. Therefore, this article uses the PCA model to build the UAV trajectory characteristics.

Authorized licensed use limited to: Pontificia Universidad Catolica de Chile. Downloaded on March 20,2025 at 19:23:50 UTC from IEEE Xplore. Restrictions apply.

For the eight indexes of x, y, z space velocity, acceleration, UAV flight direction, and curvature in UAV flight data, 100 groups of samples constitute an 11 * 100 matrix, as shown in the following formula:

$$x = \begin{bmatrix} x_{1,1} & x_{1,2} & \cdots & x_{1,8} \\ x_{2,1} & x_{2,2} & \vdots & x_{2,8} \\ \vdots & \vdots & \ddots & \vdots \\ x_{100,1} & x_{100,2} & \cdots & x_{100,8} \end{bmatrix} = \left(\vec{x_1}, \vec{x_2}, \ldots, \vec{x_8}\right). \tag{12}$$

Calculate the mean value $\overline{x_j}$ of $\vec{x_j}$ by column of matrix x, as shown in the following equation:

$$\overline{x_j} = \frac{1}{n}\sum_{i=1}^{n} x_{ij}. \tag{13}$$

Calculate its standard deviation S_j as shown in the following formula:

$$S_j = \sqrt{\frac{\sum_{i=1}^{n}\left(x_{ij} - \overline{x_j}\right)^2}{n-1}}. \tag{14}$$

Standardize the data, and the standardized data are shown in the following formula:

$$X_{ij} = \frac{x_{ij} - \overline{x_j}}{S_j}. \tag{15}$$

The standardized matrix of the original sample is obtained as shown in the following formula:

$$X = \begin{bmatrix} X_{11} & X_{12} & \cdots & X_{2p} \\ X_{21} & X_{22} & \cdots & X_{1p} \\ \vdots & \vdots & \ddots & \vdots \\ X_{n1} & X_{n2} & \cdots & X_{np} \end{bmatrix} = \left(X_1, X_2, \ldots, X_p\right). \tag{16}$$

Calculate the covariance matrix as shown in the following formula:

$$R = \begin{bmatrix} r_{11} & r_{12} & \cdots & r_{1p} \\ r_{21} & r_{22} & \vdots & r_{2p} \\ \vdots & \vdots & \ddots & \vdots \\ r_{n1} & r_{n2} & \cdots & r_{np} \end{bmatrix} \tag{17}$$

wherein r_{ij} is represented by the following formula:

$$r_{ij} = \frac{1}{n-1}\sum_{k=1}^{n}\left(X_{ki} - \overline{X_i}\right)\left(X_{kj} - \overline{X_j}\right). \tag{18}$$

The eigenvalues and eigenvectors of solving the covariance matrix R are λ_i $(i = 1, 2, \ldots, p)$ and a_i $(i = 1, 2, \ldots, p)$, respectively.

The contribution rate c_i of the ith component to the total components is defined as shown in the following formula:

$$c_i = \frac{\lambda_i}{\sum_{k=1}^{p}\lambda_k}\left(i = 1, 2, \ldots, p\right). \tag{19}$$

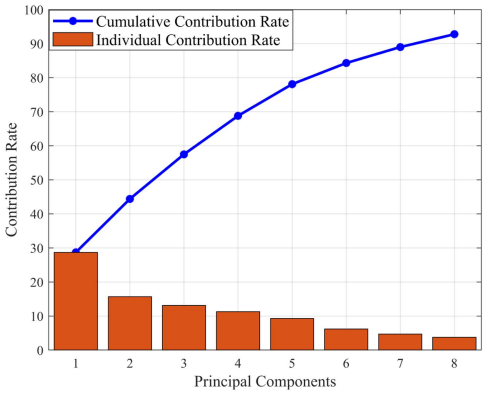

Fig. 5. UAV trajectory feature construction.

The cumulative contribution rate is defined as shown in the following equation:

$$C_i = \frac{\sum_{k=1}^{i}\lambda_k}{\sum_{k=1}^{p}\lambda_k}\left(i = 1, 2, \ldots, p\right). \tag{20}$$

Sort c_i in descending order and accumulate the cumulative contribution rate in turn. When the cumulative contribution rate exceeds 90%, it is taken as the principal component.

The main component analysis method is used to construct UAV trajectory features to improve the machine learning accuracy. The software is used to analyze the UAV trajectory characteristics, the information retention rate of the principal component is set to 90%, and the number of features is reduced to eight dimensions. Fig. 5 shows the contribution rate of a single indicator and cumulative contribution rate of UAV PCA.

As shown in Fig. 5, for the single indicator contribution rate and cumulative indicator contribution rate of UAV motion features constructed by PCA, the main components of the constructed motion features are retained, that is, the data are reduced to eight dimensions, and the cumulative contribution rate of the data is 92.7583.

B. UAV Flight Status Classification

Flight state [27] is an abstract description of different flight behaviors during UAV flight, which can be simplified into several standard states, such as climb, level flight, circle, turn, and descent [28]. Classification is one of the core issues in data mining, machine learning, and pattern recognition [29]. Common classification models include discriminant analysis, clustering analysis, SVM, etc. UAV trajectory classification is a kind of tag that predicts unknown trajectories based on trajectory learning sample training trajectory characteristics. It is widely used in target trajectorying [30], trajectory planning [31], and trajectory prediction [32]. During the navigation of UAV, the flight phase of UAV is considered as a continuous transition or combination of different flight states. The actual flight state of UAV can be obtained by identifying the flight state of UAV. The identification of UAV flight status is a necessary preparation for UAV operation analysis, an auxiliary means for UAV

Authorized licensed use limited to: Pontificia Universidad Catolica de Chile. Downloaded on March 20,2025 at 19:23:50 UTC from IEEE Xplore. Restrictions apply.

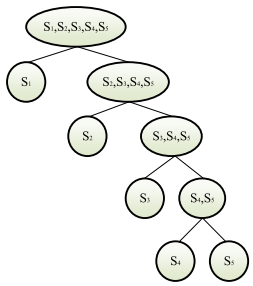

Fig. 6. Binary tree mode.

maintenance and design optimization, and has important practical value [33].

1) *UAV Flight State Classification Model:* In the literature [34], an SVM model was used to implement a multiclassification problem for detecting damage. When classifying the five flight states of the UAV, the traditional SVM model is used for classification, but the motion mode of the UAV is not a binary classification situation. Therefore, the traditional SVM model is improved and the binary tree structure is introduced to solve the defect that the SVM model can only perform binary classification [35]. In this research, the improved SVM model based on the binary tree is used to solve the problem of multiclassification recognition of UAV flight status. The SVM model separates the two types of samples by implementing high-level mapping through the kernel function. The improved SVM model through the binary tree structure can classify multiple samples one by one, so as to solve the multiclassification problem of the flight state of the UAV. The binary tree classification method for the five flight modes $S_i(i = 1, 2, 3, 4, 5)$ of the UAV is shown in Fig. 6.

As shown in Fig. 6, the improved SVM model based on binary tree can be used to recognize the five flight modes of UAV for four times.

In the SVM, for a given binary dataset $D = \{(x_i, y_i)\}_{i=1}^{N}$, where $y_i \epsilon \{+1, -1\}$, if the two samples are linearly separable, there is a hyperplane as shown in the following formula:

$$\omega^T x + b = 0. \tag{21}$$

If the two types of samples are linearly separable, then there is $y_i(\omega^T x + b) > 0$ for each sample, and the interval γ is defined as the distance from each sample in the dataset to the segmentation hyperplane, and the interval γ is shown in the following formula:

$$\gamma_i = \frac{\left|\left|\omega^T x_i + b\right|\right|}{||\omega||} \ (i = 1, 2, \ldots, N). \tag{22}$$

Define the interval γ as the shortest distance from all samples in the entire dataset to the segmented hyperplane, as shown in the following equation:

$$\gamma = \min \gamma_i \ (i = 1, 2, \ldots, N). \tag{23}$$

Data classification is achieved by finding a most suitable hyperplane. This hyperplane should satisfy the maximum interval γ, and the division of the two datasets divided by the hyperplane is the most stable and robust, that is, the optimization (24) is solved

$$\begin{cases} \max \gamma \\ \text{s.t. } \gamma_i \geq \gamma \end{cases}. \tag{24}$$

The hyperplane parameter ω of $\gamma_i = \frac{||\omega^T x_i + b||}{||\omega||} (i = 1, 2, \ldots, N)$ makes $||\omega|| \times \gamma = 1$ hold, and the optimization equation can be simplified as shown in the following equation:

$$\begin{cases} \max \frac{1}{||\omega||^2} \\ \text{s.t. } y_i \left(\omega^T x + b\right) \geq 1 \end{cases}. \tag{25}$$

For a linearly separable dataset, there are many segmentation hyperplanes, but the hyperplane with the largest interval is unique, which ensures the uniqueness of the SVM model for dataset partitioning.

2) *UAV Flight Status Classification Results:* The improved SVM model is used to identify five motion modes of UAV, including climb, level flight, circle, turn, and descent. Collect 60 groups of UAV flight data in the form of multiple indicators of multiple samples. Use 40 groups of UAV speed, acceleration, direction, and curvature of x, y, z axes under five flight states of climb, level flight, circle, turn, and descent as the training set. In total, 20 groups of data were used as test sets to verify the accuracy of the model.

In total, 40 sets of 60 sets of data are used as the training set of machine learning, and the improved SVM model is used for machine learning. In all, 20 datasets from 60 datasets are used as machine learning test sets. The 0–1 loss function is used as the loss function. The loss function between the real distribution y and the predicted distribution $f(x; \theta)$ of the label is shown in the following formula:

$$L\left(y, f\left(x; \theta\right)\right) = \begin{cases} 0 & \text{if } y = f\left(x; \theta\right) \\ 1 & \text{if } y \neq f\left(x; \theta\right) \end{cases}. \tag{26}$$

The number of classifier errors is shown in the following equation:

$$n = \sum_{i=1}^{m} \mathcal{L}\left(y_i, f_i\left(x; \theta\right)\right) \tag{27}$$

where m is the number of samples.

The correct number of classifiers is shown in the following equation:

$$r = m - n. \tag{28}$$

After calculation, the results of the five flight states classification are shown in Table III.

The accuracy of defining the classification of the classifier is shown in the following formula:

$$\gamma = \frac{m - n}{m} \times 100\%. \tag{29}$$

Formula (29) shows the number of samples and the number of classification errors.

The classification training accuracy and test accuracy of UAV in five motion states are shown in Table IV.

Authorized licensed use limited to: Pontificia Universidad Catolica de Chile. Downloaded on March 20,2025 at 19:23:50 UTC from IEEE Xplore. Restrictions apply.

TABLE III
Table of Classification Results for the Five Flight States

Flight status	Training accurate number	Testing accurate number
Climbing state	40	20
Level flight state	40	20
Circling state	39	18
Turning state	40	19
Falling state	40	20

TABLE IV
Table of Classification Accuracy for the Five Flight States

Flight status	Training accuracy %	Test accuracy %
Climbing state	100	100
Level flight state	100	100
Circling state	97.5	90
Turning state	100	95
Falling state	100	100

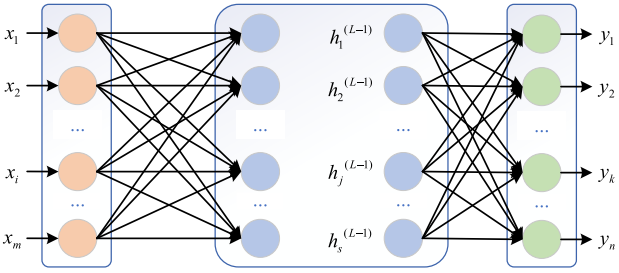

Fig. 7. BP network model.

As shown in Table IV, the SVM classifier has a good classification effect in climb, level flight, and descent recognition, and has reduced classification effect in circling motion. The classification results show that the SVM model based on the improved binary tree method is feasible in solving the multiflight mode classification problem.

IV. UAV TRAJECTORY PREDICTION MODEL

UAV trajectory prediction is a process in which UAV can predict its own trajectory in the future for a period of time through relevant algorithms based on the collected airborne information. A more accurate UAV trajectory prediction algorithm is one of the important scales for UAV self-improvement. The UAV trajectory prediction can provide theoretical support for UAV trajectory planning [36], UAV autonomous guidance [37], etc., and improve the accuracy of UAV control.

A. Back Propagation (BP) Neural Network Model

The neural network model consists of three parts: input layer, hidden layer, and output layer, and its structure is shown in Fig. 7.

As shown in Fig. 7, the neural network model first determines the number of input layers as the input parameter affecting the neural network, the middle hidden layer simulates the complex neural network of the human brain,

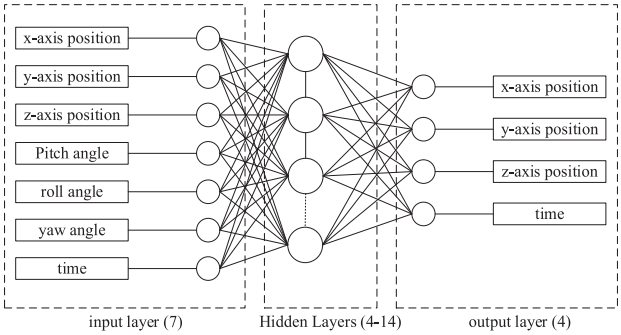

Fig. 8. BP network topology.

and finally outputs the prediction of the input layer at the output layer.

The propagation process of the BP mathematical modeling algorithm includes two aspects: the forward propagation of information in the input layer and the back propagation of error in the output layer.

1) *Forward Propagation:* The BP neural network consists of an input layer, a hidden layer, and an output layer. By passing the data weighting operation of the input layer to the hidden layer, and then passing the data weighting operation of the hidden layer to the output layer, the neural network information is realized. Forward propagation. The output results z_k and y_j of the hidden layer node and the output layer node are shown in (30) and (31), respectively

$$z_k = f_1\left(\sum_{i=0}^{n} v_{ki}x_i\right) \quad k = 1, 2, \ldots, q \tag{30}$$

$$y_j = f_2\left(\sum_{k=0}^{q} w_{jk}x_i\right) \quad j = 1, 2, \ldots, m. \tag{31}$$

where f_1 and f_2 are the transfer functions from the input layer to the hidden layer and from the hidden layer to the output layer, respectively; n, q, and m are the number of nodes in the input layer and the output layer of the hidden layer, respectively; and v_{ki} and w_{jk} are the weights of the input layer and the hidden layer, the hidden layer and the output layer, respectively.

2) *Back Propagation:* The neural network adopts the stochastic gradient descent method to learn the neural network parameters. For the given ith sample (x_i, y_i), input the sample into the neural network model, and the obtained network output is shown in the following formula:

$$\hat{y}_i = f(x_i; \theta) \tag{32}$$

where x_i is the column vector input by the samples in the ith group, θ is the learning criterion, and $\hat{y}_i$ is the column vector input by the samples in the group.

a) *Loss function:* The loss function is a nonnegative real function that quantifies the difference between the model predictions and the true labels. The loss function is defined as a square loss function as shown in the following equation:

$$\varepsilon(y_i, \hat{y}_i) = \frac{1}{2}(y_i - \hat{y}_i)^2. \tag{33}$$

Authorized licensed use limited to: Pontificia Universidad Catolica de Chile. Downloaded on March 20,2025 at 19:23:50 UTC from IEEE Xplore. Restrictions apply.


Fig. 9. UAV flight information measurement photographs.

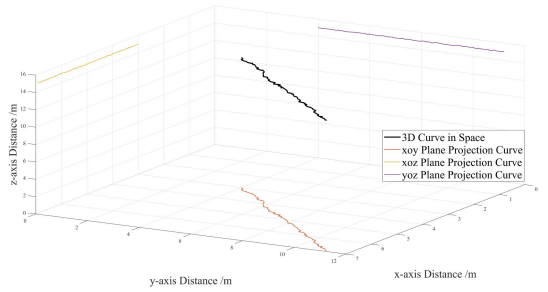

Fig. 10. UAV trajectory in flat flight.

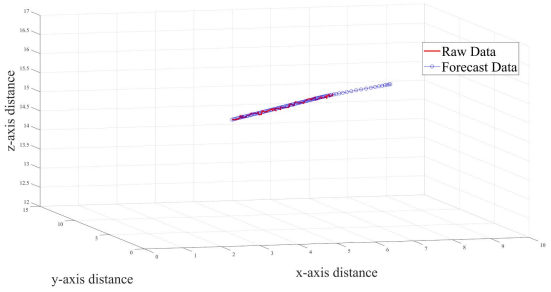

Fig. 11. Level flight state trajectory prediction map.

TABLE V
Neural Network Parameter Setting Table

Parameter name	Number of settings
The number of training set samples	80
The number of samples in the test set	20
Learning rate	0.001
Enter the number of nodes	7
Number of hidden layer nodes	8
Number of output nodes	4
Activation function	sigmoid

The total error generated for the p group of neural network samples can be defined as shown in the following formula:

$$E_p = \frac{1}{2}\sum_{i=1}^{p}\left(y_i - \hat{y}_i\right)^2. \tag{34}$$

b) *Empirical risk minimization:* The smaller the loss predicted by the model, the stronger the prediction ability of the model. In order to obtain a smaller expected error, the empirical risk is calculated, that is, the average loss of the training set is shown in the following formula:

$$R(\theta) = \frac{1}{N}\sum_{i=1}^{N}\varepsilon\left(y_i, f(x_i;\theta)\right). \tag{35}$$

Algorithm 1: Stochastic Gradient Descent.

in put: training dataset $D = \{x_i, y_i\}_{i=1}^{N}$, validation dataset V, learning rate α

1 random initialization

2 repeat

3 Randomly sort the training dataset D samples

4 for i=1…N do

5 Select sample (x_i, y_i) from training dataset D

6 $\theta \leftarrow \theta - \alpha\dfrac{\partial\varepsilon(\theta; x_i, y_i)}{\partial\theta}$

7 end

8 until $f(x_i;\theta)$ has the lowest error rate on validation dataset V

Out put θ

c) *Stochastic gradient descent:* Find a suitable learning criterion θ to minimize the empirical risk to solve the model parameters. The empirical risk function is a nonconvex function constructed as the optimization target, and the stochastic gradient descent method is used to optimize the empirical risk function. The training of the stochastic gradient descent method process is shown in Algorithm 1.

As shown in Algorithm 1, the training process of stochastic gradient descent is described. After enough iterations, stochastic gradient descent will converge to a local optimal solution.

B. UAV Trajectory Prediction

The UAV operating state data is collected in different operating states as a neural network training dataset. After the neural network is trained, it will predict the future flight path according to the current operating state and current flight path information. The flight state of the UAV is divided into five kinds, and the corresponding neural network is trained for the five flight states to predict the flight path of the UAV under the motion state. The trajectory prediction model established in this article is used for trajectory prediction of small UAVs, and the topology of the BP network is shown in Fig. 8.

As shown in Fig. 8, the UAV trajectory prediction neural network selects seven inputs and four outputs. The seven inputs are, respectively, the position (longitudinal displacement, lateral displacement, vertical displacement), angular motion parameters (pitch angle, roll angle, yaw angle), and heading in the direction of the x, y, z coordinate axis. The four outputs are displacement changes and time in the x, y, and z directions, respectively, to describe the 4-D flight path of the UAV.

The number of hidden nodes will affect the prediction effect of neural network. A small number of nodes will reduce the fault tolerance of the network model and affect the prediction results. A large number of nodes will also reduce the prediction ability, resulting in a long calculation time. The empirical formula and the formula for determining the hidden layer node of the sum of error squares are

Authorized licensed use limited to: Pontificia Universidad Catolica de Chile. Downloaded on March 20,2025 at 19:23:50 UTC from IEEE Xplore. Restrictions apply.

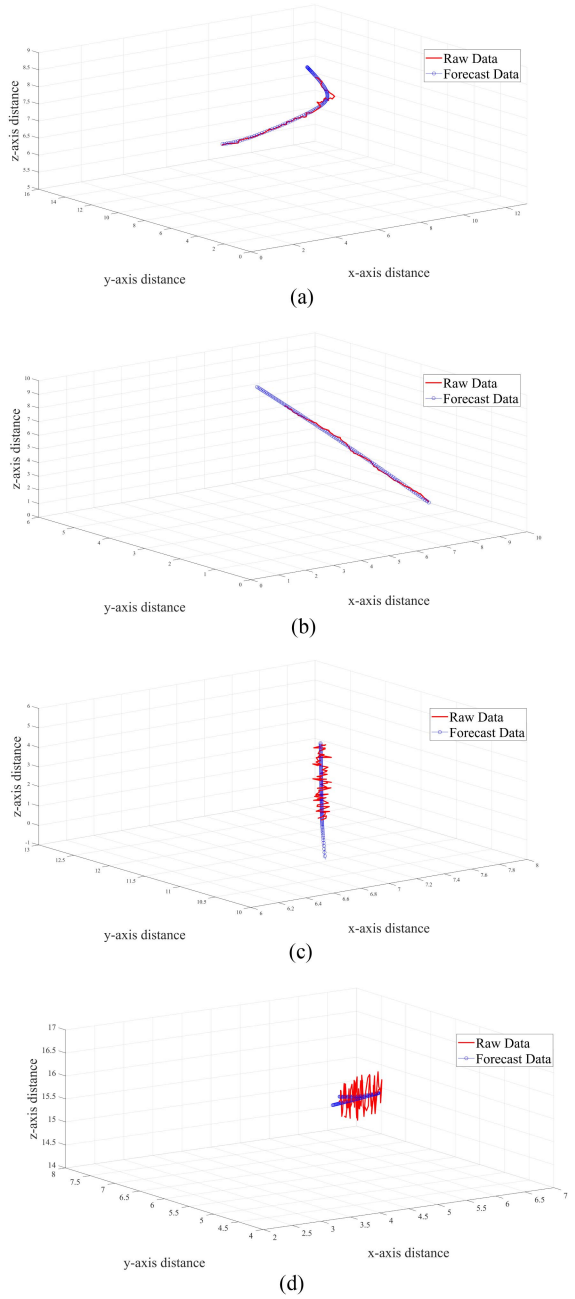

Fig. 12. Prediction charts of UAV trajectories in four flight states. (a) Turning state trajectory prediction diagram. (b) Climb state trajectory prediction chart. (c) Descent state trajectory prediction diagram. (d) Circling state trajectory prediction map.

shown in the following formula:

$$S = \sqrt{U + V} + a \tag{36}$$

where S is the number of hidden layer nodes, U is the number of input nodes, V is the number of output nodes, and a represents an integer of [1,10].

The range of the number of hidden layer nodes is calculated as follows: $H = \sqrt{7+4} + [1, 10] = [4, 14]$.

V. EXPERIMENTAL RESULTS AND ANALYSIS

In this experiment, we measured the flight information of the UAV using the device shown in Fig. 1. At the same time, we recorded the data of the UAV flight, and the measurement of the UAV flight process is shown in Fig. 9.

In this article, the environment is MATLAB 2019a, and the computer configuration used is i7-9750H CPU, 8 GB RAM.

In neural network training, the sample dataset needs to be divided into a training set and a test set, the training set is used for training the neural network, and the test set is used to evaluate the quality of the trained neural network. In this neural network sample set, 100 groups of samples were collected for each of the five motion modes. According to the neural network training principle, the training set was divided into 80 groups of samples, and the test set was divided into 20 groups of samples for neural network training. To obtain a reliable model, the learning rate lr is selected to be 0.001 through multiple trials and experience. The parameters of the prediction model and initial configuration are shown in Table V.

As shown in Table V, the basic parameters set by the neural network are set. After setting the network parameters, the flight path prediction is performed using the data returned by the UAV.

A. Prediction Results

To collect UAV flight data, first perform data preprocessing, and then use PCA-SVM to classify the flight state, and select one of the UAV flight data identified as level flight state, as shown in Fig. 10.

As shown in Fig. 10, the navigation data of the UAV in the state of level flight are described. The neural network model corresponding to the level flight state is used to predict the UAV trajectory, and the 3-D trajectory prediction diagram of the UAV is drawn, as shown in Fig. 11.

As shown in Fig. 11, the 3-D trajectory of the UAV predicted under the corresponding neural network in the level flight state is described. The red solid line describes the initial trajectory curve of the UAV, and the blue circle describes the neural network of the UAV. The network fits the predicted trajectory curve, and the density of the circles describes the speed of the UAV in space. You can see the predicted blue line type and red line type that you are in good shape.

The navigation data identified as the four motion states of UAV turning, climbing, descending, and circling are, respectively, selected and their corresponding neural network prediction trajectories are shown in Fig. 12(a)–(d).

As shown in Fig. 12(a)–(d) describe the 4-D trajectory and its predicted trajectory of the UAV in the turning, climbing, descending, and circling states, respectively. The red solid line describes the UAV. The actual trajectory curve, the blue circle-shaped line describes the predicted trajectory curve fitted by the UAV neural network, and the density of the circle describes the speed of the UAV in space. Combining with Fig. 9, it can be seen that in the fitting effect of the neural network corresponding to the five motion states to the real trajectory of the UAV, the fitting effect of the level

Authorized licensed use limited to: Pontificia Universidad Catolica de Chile. Downloaded on March 20,2025 at 19:23:50 UTC from IEEE Xplore. Restrictions apply.

flight, turning, climbing, and descending states is good, and the fitting effect of the circling state is general.

B. Analysis of Experimental Results

1) *Neural Network Analysis:* The neural network is trained repeatedly to achieve the minimum mean square error (MSE) through function transfer and model fitting. The cross-validation graph describes the MSE performance of each generation and the training algebra of the optimal MSE in the neural network training process; regression coefficient is used to describe the regression ability of the network training set, verification set, and test set. The closer the regression coefficient is to 1, the better the effect is. As shown in Fig. 13, the neural network cross-validation diagram under five motion states and the regression coefficient R of the neural network are described.

As shown in Fig. 13, the minimum training MSE error in the descending state neural network is 0.001211 and the maximum regression coefficient is 0.9996. The maximum training MSE error in the circling state neural network is 0.25799 and the maximum regression coefficient in the level flight state is 0.99945.

2) *Forecast Result Analysis:* The accuracy of network prediction is verified by the actual trajectory and predicted trajectory of UAV during flight, and the necessity of flight state recognition in trajectory prediction is determined by comparing the effect of predicting UAV's trajectory directly using a neural network with that of predicting UAV's trajectory after flight state recognition. Taking the turning state as an example, the two prediction results are shown in Fig. 14.

Fig. 14 shows the predicted trajectory of the UAV and the real trajectory of the UAV under turning state. It can be seen that the error of prediction directly using a neural network is far greater than the error of prediction using a neural network after flight state recognition. It can be seen that flight state recognition can effectively improve the accuracy of UAV prediction before UAV trajectory prediction.

The distance d between the predicted trajectory point and the actual trajectory point is defined as shown in the following formula:

$$d = \sqrt{(x-\hat{x})^2 + \left(y-\hat{y}\right)^2 + (z-\hat{z})^2} \tag{37}$$

where x represents the x-axis distance of the UAV's actual trajectory, $\hat{x}$ represents the x-axis distance of the UAV's predicted trajectory, y represents the y-axis distance of the UAV's actual trajectory, $\hat{y}$ represents the y-axis distance of the UAV's predicted trajectory, z represents the z-axis distance of the UAV's actual trajectory, and $\hat{z}$ represents the z-axis distance of the UAV's predicted trajectory.

The average value of the Euclidean distance between the predicted trajectory and the actual trajectory at each time point is taken as the error distance of trajectory prediction. The error distance μ of the predicted trajectory is shown in the following formula:

$$\mu = \frac{1}{N}\sum_{i=1}^{N} d_i = \sqrt{(x_i-\hat{x}_i)^2 + \left(y_i-\hat{y}_i\right)^2 + (z_i-\hat{z}_i)^2} \tag{38}$$

where N represents the number of trajectory points.

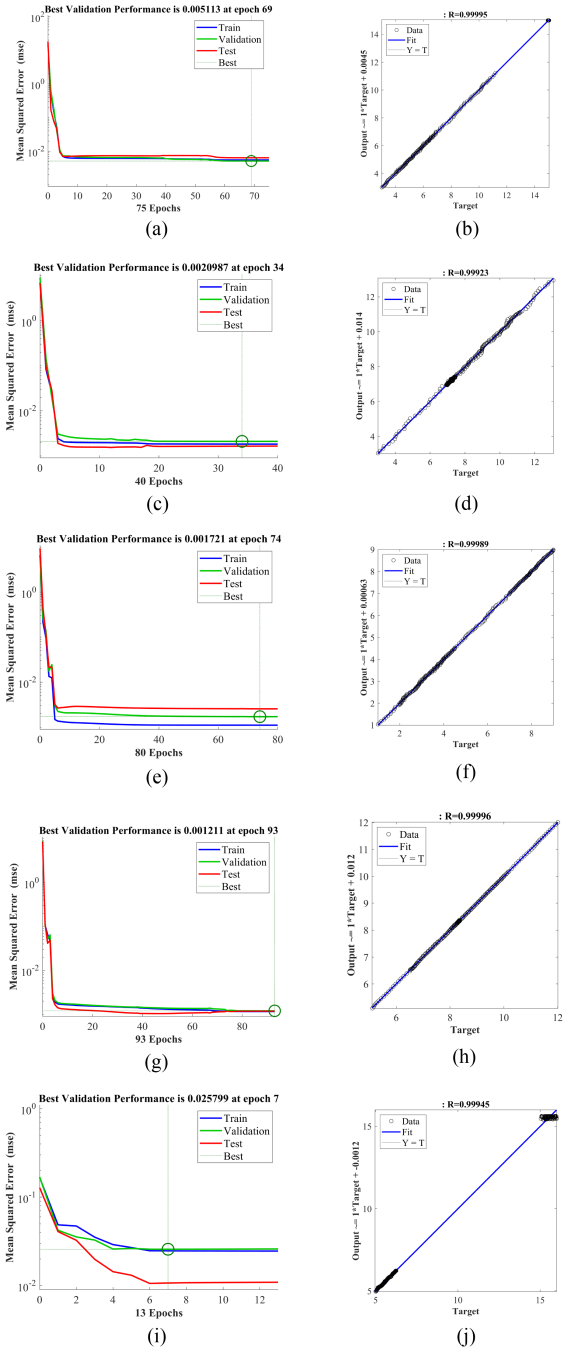

Fig. 13. Neural network analysis chart. (a) Iterative performance diagram of level flight state. (b) Regression diagram of level flight network. (c) Iterative performance graph of turning state. (d) Regression graph of turning state network. (e) Iterative performance diagram of climbing state. (f) Regression graph of climbing state network. (g) Iterative performance diagram of descending state. (h) Regression graph of descending state network. (i) Iterative performance graph of circling state. (j) Regression graph of circling state network.

Authorized licensed use limited to: Pontificia Universidad Catolica de Chile. Downloaded on March 20,2025 at 19:23:50 UTC from IEEE Xplore. Restrictions apply.

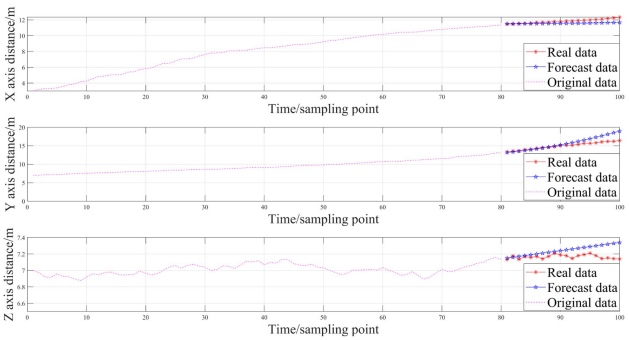

(a)

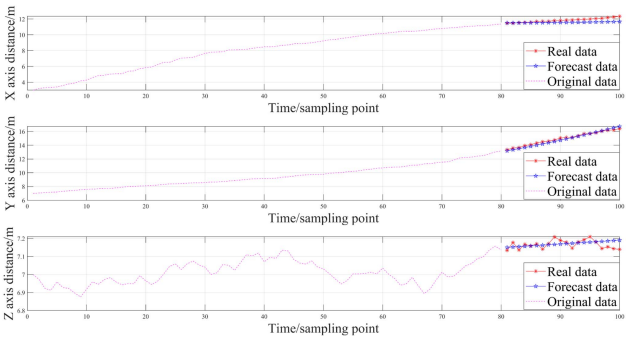

(b)

Fig. 14. Effect of trajectory prediction. (a) Effect diagram of direct BP neural network prediction. (b) Effect diagram of BP neural network prediction after flight status recognition.

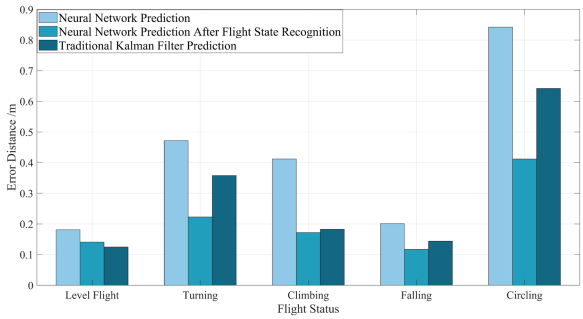

Fig. 15. UAV trajectory prediction error diagram.

The trajectory error predicted directly by the neural network for each of the five flight states, the trajectory error predicted by the neural network after flight state identification, and the trajectory error predicted by the conventional Kalman filter method are shown in Fig. 15.

As shown in Fig. 15, compared with the traditional neural network prediction, the neural network prediction error after flight state recognition has significantly decreased, especially in the circling state. After flight state identification, the UAV prediction error is the smallest in descending state, with an error distance of 0.13 m, and the UAV prediction error is the largest in the circling state, with an error distance of 0.41 m. After flight status recognition, the UAV trajectory prediction error is controlled within 0.5 m. At the same time, the traditional Kalman filter method has a higher prediction accuracy than the traditional neural network model. The error of the traditional Kalman filter method is only slightly smaller than that of the UAV trajectory prediction model based on flight state recognition proposed in this article in the level flight state, and the prediction error of the traditional Kalman filter method is larger than that of the UAV trajectory prediction model based on flight state recognition proposed in this article in all other flight states. Tests show that the UAV trajectory prediction model based on flight state recognition can realize the UAV trajectory prediction. Compared with the traditional Kalman filter prediction method, the UAV trajectory prediction model based on flight state recognition proposed in this article is more accurate.

VI. CONCLUSION

In this article, the UAV trajectory prediction model is established for different flight states. First, data preprocessing is carried out, including abnormal data elimination and missing data interpolation; second, the UAV flight state recognition model is established; and finally, a neural network model of five flight states is established based on BP neural network for trajectory prediction. The following conclusions can be drawn from the experiment.

1) The classification accuracy of five flight states of UAVs is higher than 90%, and the PCA-SVM-based UAV flight state recognition model is feasible.
2) The UAV flight state recognition can improve the accuracy of UAV prediction. The experimental data shows that the UAV trajectory error predicted by this method can be controlled within 0.5 m.
3) Compared with the traditional neural network prediction model, the prediction accuracy of the neural network model based on UAV flight state recognition has been improved to varying degrees in the five flight states.
4) The proposed UAV trajectory prediction model based on flight state recognition in this article is more effective than the conventional UKF method in predicting the UAV trajectory in this experimental setting.

The proposed UAV trajectory prediction method is mainly used for UAV trajectory prediction during autonomous flight. A more accurate trajectory prediction method is more helpful for the improvement of UAV autonomous flight capability.

In future research, we will consider trajectory prediction in UAV cluster collaboration. In addition, the flight states in this article are the result of deep learning; it needs a lot of human experience to assist the model's judgment. In future research, we will consider selecting suitable metrics based on deep reinforcement learning for research in this area.

Authorized licensed use limited to: Pontificia Universidad Catolica de Chile. Downloaded on March 20,2025 at 19:23:50 UTC from IEEE Xplore. Restrictions apply.

REFERENCES

[1] E. Kakaletsis et al., "Computer vision for autonomous UAV flight safety: An overview and a vision-based safe landing pipeline example," *ACM Comput. Surv.*, vol. 54, no. 9, pp. 1–37, Dec. 2022, doi: 10.1145/3472288.

[2] C. Yan, L. Fu, X. Luo, and M. Chen, "A brief overview of waveforms for UAV air-to-ground communication systems," in *Proc. 3rd Int. Conf. Vision, Image Signal Process.*, Vancouver, BC, Canada, 2019, pp. 1–7, doi: 10.1145/3387168.3387203.

[3] D. Orfanus, E. P. de Freitas, and F. Eliassen, "Self-organization as a supporting paradigm for military UAV relay networks," *IEEE Commun. Lett.*, vol. 20, no. 4, pp. 804–807, Apr. 2016.

[4] H. Shakhatreh et al., "Unmanned aerial vehicles: A survey on civil applications and key research challenges," *IEEE Access*, vol. 7, pp. 48572–48634, 2019.

[5] M. Sherman, M. Gammill, A. Raissi, and M. Hassanalian, "Solar UAV for the inspection and monitoring of photovoltaic (PV) systems in solar power plants," in *Proc. Amer. Inst. Aeronaut. Astronaut. SciTech Forum*, Jan. 2021.

[6] A.-I. Siean, R.-D. Vatavu, and J. Vanderdonckt, "Taking that perfect aerial photo: A synopsis of interactions for drone-based aerial photography and video," in *Proc. ACM Int. Conf. Interactive Media Experiences*, 2021, pp. 275–279, doi: 10.1145/3452918.3465484.

[7] Y. Xia, G. Ye, S. Yan, Z. Feng, and F. Tian, "Application research of fast UAV aerial photography object detection and recognition based on improved YOLOv3," *J. Phys., Conf. Ser.*, vol. 1550, no. 3, May 2020, Art. no. 032075, doi: 10.1088/1742-6596/1550/3/032075.

[8] Y. Liu and S. Liu, "Design and implementation of farmland environment monitoring system based on micro quadrotor UAV," *J. Phys., Conf. Ser.*, vol. 2281, no. 1, Jun. 2022, Art. no. 012005, doi: 10.1088/1742-6596/2281/1/012005.

[9] M. Zhang, H. Wang, and J. Wu, "On UAV source seeking with complex dynamic characteristics and multiple constraints: A cooperative standoff monitoring mode," *Aerosp. Sci. Technol.*, vol. 121, Feb. 2022, Art. no. 107315, doi: 10.1016/j.ast.2021.107315.

[10] M. Corbetta, P. Banerjee, W. Okolo, G. Gorospe, and D. G. Luchinsky, "Real-time UAV trajectory prediction for safety monitoring in low-altitude airspace," in *Proc. Amer. Inst. Aeronaut. Astronaut. Aviation Forum*, Jun. 2019.

[11] P. Banerjee and M. Corbetta, "Uncertainty quantification of expected time-of-arrival in UAV flight trajectory," in *Proc. Amer. Inst. Aeronaut. Astronaut. Aviation Forum*, Aug. 2021.

[12] M. Zwick, M. Gerdts, and P. Stütz, "Sensor model-based trajectory optimization for UAVs using nonlinear model predictive control," in *Proc. Amer. Inst. Aeronaut. Astronaut. Scitech Forum*, Jan. 2022.

[13] Z. Wang, G. Zhang, B. Hu, and X. Feng, "Real time detection and identification of UAV abnormal trajectory," in *Proc. 3rd Int. Conf. Artif. Intell. Pattern Recognit.*, Xiamen, China, 2020, pp. 51–56, doi: 10.1145/3430199.3430212.

[14] H. G. de Marina, F. Espinosa, and C. Santos, "Adaptive UAV attitude estimation employing unscented Kalman filter, FOAM and low-cost MEMS sensors," *Sensors*, vol. 12, no. 7, pp. 9566–9585, Jul. 2012, doi: 10.3390/s120709566.

[15] R. Kannan, "Orientation estimation based on LKF using differential state equation," *IEEE Sensors J.*, vol. 15, no. 11, pp. 6156–6163, Nov. 2015.

[16] G. Heredia, A. Duran, and A. Ollero, "Modeling and simulation of the HADA reconfigurable UAV," *J. Intell. Robot. Syst.*, vol. 65, no. 1–4, pp. 115–122, Jan. 2012, doi: 10.1007/s10846-011-9561-9.

[17] D. Thipphavong and C. Schultz, "The effect of rate-of-climb uncertainty on an adaptive trajectory prediction algorithm for climbing flights," in *Proc. 12th Amer. Inst. Aeronaut. Astronaut. Aviation Technol., Integr., Oper. Conf./14th AIAA/ISSMO Multidisciplinary Anal. Optim. Conf.*, Sep. 2012.

[18] H. Zhang, Y. Yan, S. Li, Y. Hu, and H. Liu, "UAV behavior-intention estimation method based on 4-D flight-trajectory prediction," *Sustainability*, vol. 13, no. 22, Nov. 2021, Art. no. 12528, doi: 10.3390/su132212528.

[19] Z. Niu, X. Jia, and W. Yao, "Communication-free MPC-based neighbors trajectory prediction for distributed multi-UAV motion planning," *IEEE Access*, vol. 10, pp. 13481–13489, 2022.

[20] R. Alligier and D. Gianazza, "Learning aircraft operational factors to improve aircraft climb prediction: A large scale multi-airport study," *Transp. Res. Part C, Emerg. Technol.*, vol. 96, pp. 72–95, Nov. 2018, doi: 10.1016/j.trc.2018.08.012.

[21] B. Wang, D. Liu, W. Wang, and X. Peng, "A hybrid approach for UAV flight data estimation and prediction based on flight mode recognition," *Microelectron. Rel.*, vol. 84, pp. 253–262, May 2018, doi: 10.1016/j.microrel.2018.03.032.

[22] B. Kada, K. Munawar, M. S. Shaikh, M. A. Hussaini, and U. M. Al-Saggaf, "UAV attitude estimation using nonlinear filtering and low-cost MEMS sensors," *IFAC-PapersOnLine*, vol. 49, no. 21, pp. 521–528, 2016, doi: 10.1016/j.ifacol.2016.10.655.

[23] G. Zhong, H. Zhang, J. Zhou, J. Zhou, and H. Liu, "Short-term 4D trajectory prediction for UAV based on spatio-temporal trajectory clustering," *IEEE Access*, vol. 10, pp. 93362–93380, 2022.

[24] Y. Liu, H. Wang, J. Fan, J. Wu, and T. Wu, "Control-oriented UAV highly feasible trajectory planning: A deep learning method," *Aerosp. Sci. Technol.*, vol. 110, Mar. 2021, Art. no. 106435, doi: 10.1016/j.ast.2020.106435.

[25] G. Xie and X. Chen, "Efficient and robust online trajectory prediction for non-cooperative unmanned aerial vehicles," *J. Aerosp. Inf. Syst.*, vol. 19, no. 2, pp. 143–153, Feb. 2022, doi: 10.2514/1.I010997.

[26] W. Jia, M. Sun, J. Lian, and S. Hou, "Feature dimensionality reduction: A review," *Complex Intell. Syst.*, vol. 8, no. 3, pp. 2663–2693, Jun. 2022, doi: 10.1007/s40747-021-00637-x.

[27] H.-J. Jeong, S.-Y. Choi, S.-S. Jang, and Y.-G. Ha, "Probability machine-learning-based communication and operation optimization for cloud-based UAVs," *J. Supercomput.*, vol. 76, no. 10, pp. 8101–8117, Oct. 2020, doi: 10.1007/s11227-018-2728-4.

[28] A. Giagkos, E. Tuci, M. S. Wilson, and P. B. Charlesworth, "UAV flight coordination for communication networks: Genetic algorithms versus game theory," *Soft Comput.*, vol. 25, no. 14, pp. 9483–9503, Jul. 2021, doi: 10.1007/s00500-021-05863-6.

[29] M. Lochner and B. Bassett, "Machine learning for transient classification: Workshop 13," *Proc. Int. Astronomical Union*, vol. 14, no. S339, pp. 274–274, Nov. 2017, doi: 10.1017/S1743921318002740.

[30] Y. Song, Z. Hu, T. Li, and H. Fan, "Performance evaluation metrics and approaches for target trajectorying: A survey," *Sensors*, vol. 22, no. 3, Jan. 2022, Art. no. 793, doi: 10.3390/s22030793.

[31] X. Niu, X. Yuan, Y. Zhou, and H. Fan, "UAV trajectory planning based on evolution algorithm in embedded system," *Microprocessors Microsyst.*, vol. 75, Jun. 2020, Art. no. 103068, doi: 10.1016/j.micpro.2020.103068.

[32] Q. Yang, Z. Ye, X. Li, D. Wei, S. Chen, and Z. Li, "Prediction of flight status of logistics UAVs based on an information entropy radial basis function neural network," *Sensors*, vol. 21, no. 11, May 2021, Art. no. 3651, doi: 10.3390/s21113651.

[33] R. K. Mehra, S. Seereeram, J. T. Wen, and D. S. Bayard, "Nonlinear predictive control for spacecraft trajectory guidance, navigation and control," in *Proc. Amer. Inst. Phys. Conf.*, Albuquerque, NM, USA, 1998, vol. 420, pp. 147–152, doi: 10.1063/1.54919.

[34] Z. Wang and Y.-J. Cha, "Unsupervised deep learning approach using a deep auto-encoder with a one-class support vector machine to detect damage," *Struct. Health Monit.*, vol. 20, no. 1, pp. 406–425, Jan. 2021, doi: 10.1177/1475921720934051.

[35] W. Li, L. Wang, L. Zhang, and J. Liu, "A multi-fault classification algorithm based on improved binary tree support vector machines," *J. Detection Control*, vol. 37, no. 3, pp. 34–39, Jun. 2015.

[36] D. González-Arribas, M. Soler, and M. Sanjurjo-Rivo, "Robust aircraft trajectory planning under wind uncertainty using optimal control," *J. Guid., Control, Dyn.*, vol. 41, no. 3, pp. 673–688, Mar. 2018, doi: 10.2514/1.G002928.

Authorized licensed use limited to: Pontificia Universidad Catolica de Chile. Downloaded on March 20,2025 at 19:23:50 UTC from IEEE Xplore. Restrictions apply.

[37] N. Dadkhah and B. Mettler, "Survey of motion planning literature in the presence of uncertainty: Considerations for UAV guidance," *J. Intell. Robot. Syst.*, vol. 65, no. 1–4, pp. 233–246, Jan. 2012, doi: 10.1007/s10846-011-9642-9.

Jiandong Zhang received the bachelor's degree in fire control, master's degree in system engineering, and doctor's degree in system engineering from the Northwestern Polytechnical University, Xi'an, China, in 1997, 2000, and 2005, respectively.

From 2005 to 2007, he was engaged in research in the postdoctoral mobile station of information and communication engineering of the University. In 2007, he was promoted to Associate Professor of system engineering discipline of the Northwestern Polytechnical University. Since 2007, he has been serving as the tutor of master's degree.

Dr. Zhang is a member of the China System Simulation Society.

Zhuoyong Shi was born in Shaanxi Province, China, in 2001. He received the bachelor's degree in electronic information engineering from Xi'an Jiaotong University City College, Xi'an, China, in 2022. Since 2022, he has been working toward the master's degree in electronic science and technology with the Northwestern Polytechnical University, Xi'an, China.

Anli Zhang received the bachelor's degree in electronic engineering from Shaanxi Institute of Technology, Xi'an, China, in 1998, and the master's degree in system engineering from Northwestern Polytechnical University, Xi'an, in March 2006.

Since 2006, she has been engaged in the teaching and research of electronic information engineering with Xi'an Jiaotong University City College, Xi'an. In 2018, she was promoted to the Professor of electronic science and technology discipline at Xi'an Jiaotong University City College, where in 2023, she was promoted to the Professor of electronic science and technology discipline.

Qiming Yang received the bachelor's degree in detection guidance and control technology, the master's degree in system engineering, and the doctor's degree in electronic science and technology from Northwestern Polytechnical University, Xi'an, China, in 2010, 2013, and 2020, respectively.

Guoqing Shi received the bachelor's degree in automatic control from Lanzhou Jiaotong University, Lanzhou, China, in 1997, and the master's degree in system engineering in 2004 and doctor's degree in system engineering in 2011 from Northwestern Polytechnical University, Xi'an, China.

He was promoted to Associate Professor of system engineering discipline of Northwestern Polytechnical University.

Yong Wu received the bachelor's degree in fire control and master's degree in system engineering from Northwestern Polytechnical University, Xi'an, China, in 1985 and 1988, respectively.

He was promoted to Professor of system engineering discipline of Northwest Polytechnical University.

Authorized licensed use limited to: Pontificia Universidad Catolica de Chile. Downloaded on March 20,2025 at 19:23:50 UTC from IEEE Xplore. Restrictions apply.